Numerical Calculation of Energy Release Rates by Virtual Crack Closure Technique

Yoon-Suk Chang*, Jae-Boong Choi, Young-Jin Kim
SAFE Research Centre, School of Mechanical Engineering, Sungkyunkwan University, 300 Chunchun-dong, Jangan-gu, Suwon, Kyonggi-do 440-746, Korea
Genki Yagawa
Department of Quantum Engineering & System Science University of Tokyo, 7-3-1 Hongo, Bunkyo-ku, Tokyo 113-8656, Japan

A seamless analysis of material behavior incorporating complex geometry and crack- tip modeling is one of greatly interesting topics in engineering and computational fracture mechanics fields. However, there are still large gaps between the industrial applications and fundamental academic studies due to a time consuming detailed modeling. In order to resolve this problem, a numerical method to calculate an energy release rate by virtual crack closure technique was proposed in this paper. Both free mesh method and finite element method have been utilized and, thereafter, robust local and global elements for various geometries and boundary conditions were generated. A validity of the proposed method has been demonstrated through a series of fracture mechanics analyses without tedious crack-tip meshing.

Key Words: Free Mesh Method, Finite Element Method, Energy Release Rate, Stress Intensity Factor, Virtual Crack Closure Technique

1. Introduction

The recent progress of computational mechanics has promoted the wide utilization of finite element method (FEM) and alternatives in various fields and extended the practicality to complex geometries using unstructured computational grids. However, large gaps between the industrial applications and fundamental academic studies still exist. The primary reason is that the existing numerical methods have a weak point in detailed modeling required for practical engineering application. For example, how to model three-dimensional complex boundary shapes or objects that contain lots of cracks or discontinuities is remained as a representative unsettled problem. During the last two decades, in order to resolve the problem, several mesh-free methods have been proposed. Some of the mesh-free methods, in spite of the original features, adopt seamless computing techniques firmly binding to FEM instead of other approximation techniques or formula for specific evaluation (Melenk and Babuska, 1996; Belytschko and Black, 1999; Belytschko et al., 1999; Jin and Suzuki, 2000; Choi and Kim, 2003; Cho and Jee, 2003). Here, the seamless techniques focus on a close relationship between the numerical simulation and CAD or various image input data.

The objective of this paper is to introduce promising numerical methods to calculate energy release rates, which are simple but suitable for seamless computing as well as a series of numerical analyses. In this paper, for numerical calculation of energy release rates, both free mesh method (FMM) and FEM are utilized and a virtual

* Corresponding Author,
E-mail: yschang7@skku.edu
TEL: +82-31-290-7459; **FAX**: +82-31-290-5276
SAFE Research Centre, School of Mechanical Engineering, Sungkyunkwan University, 300 Chunchun-dong, Jangan-gu, Suwon, Kyonggi-do 440-746, Korea.
(Manuscript **Received** June 15, 2004; **Revised** August 11, 2004)

crack closure technique (VCCT) that does not require tedious crack-tip singular elements is adopted. The FMM can be called as a node-based FEM in which a local mesh generation technique is employed. Thereby, robust local elements for complex geometries and/or boundary conditions are generated while maintaining sufficient efficiency. For the seamless computing, triangular elements in case of two-dimensional analyses and tetrahedral elements in case of three-dimensional analyses are used since it is convenient for automatic mesh generation. Several case studies on linear elastic fracture mechanics (LEFM) problems using the proposed methods have been carried out to check the applicability incorporating the immanent limitation of the element types.

The remainder of this paper is organized as follows. In Section 2, an algorithm of local mesh generation and system construction by the proposed FMM is presented. In Section 3, technical backgrounds of VCCT are surveyed and details of applicability as well as a basic concept are reviewed. In Section 4, numerical examples of two-dimensional crack propagation analyses using FMM and three-dimensional stable crack analyses using FEM are presented and further research items are discussed. Finally, in Sections 5, conclusions of this paper are derived.

2. Free Mesh Method

2.1 Algorithm of local mesh generation

The FEM has obviously a dominant status in the field of computational methods in engineering, mostly because of its greater flexibility and wider range of applicability. On the contrary, the development of alternative methods that do not require the generation of a mesh for complicated domains is still very appealing. The current problem of mesh generation is that the time remains unbounded even using the most sophisticated mesh generator. Several computational mesh-free methods have been proposed to overcome the troublesome process in mesh generation for structural analysis. However, those have not been succeeded in completely replacing the FEM whilst the methods exhibit excellent performance in some specific fields. In order to resolve the problems, recently, FEM-based mesh-free methods have been reported. The FMM introduced in this paper is one of the mesh-free methods and has been progressed continuously from the original one (Yagawa and Yamada, 1996 ; Yagawa and Furukawa, 2000 ; Inaba et al., 2002).

The key procedure of FMM is as follows: It starts from distributing nodes appropriately across concerned analysis domain. Data inputs of this method are surface patches and nodes as depicted in Fig. 1. The surface patches are defined as sets of segments in two-dimensional space or sets of planes in three-dimensional space, which surround the analysis domain and depict the shape of domain. Fig. 2 illustrates data structure of the proposed method. At first, a single node P_i among the distributed nodes is designated as a central node. And then, a local mesh is generated around the central node P_i based on local Delaunay triangulation algorithm based on gift-wrapping technique (Inaba et al., 2002). The gift-wrapping technique is an algorithm that calculates a triangle of Delaunay triangulation in a one-by-one manner. Therefore, it is well suited to massively parallel computing, because the algorithm is highly localized spatially. The local meshes can always be generated by minimum searching of nodes without needing searching circles when this method is applied to local mesh

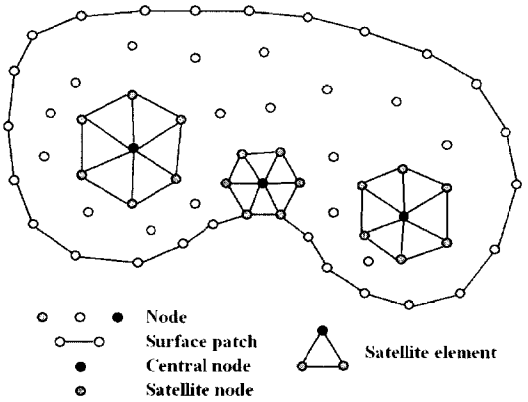

Fig. 1 Definition of surface patch and nodes

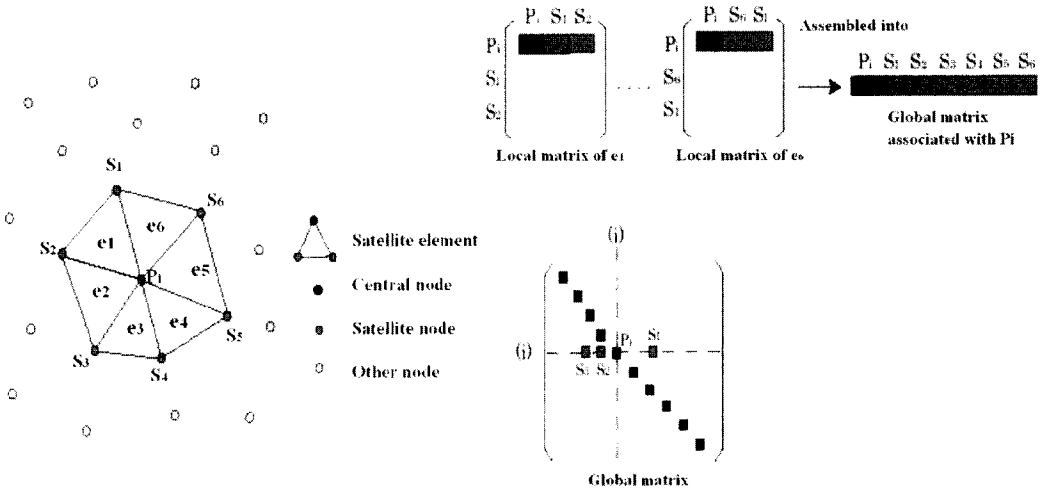

Fig. 2 Data structure of FMM

generation. Furthermore, the algorithm can generate local meshes robustly while maintaining the extreme geometry of an object, even if the object contains knife-edge geometries.

Elements formed by the local mesh generation technique are classified as satellite elements that are associated with the P_i. Corresponding nodes of the satellite elements are referred to satellite nodes against the central node. These local meshes around each node should be generated under the premises that edges of satellite elements do not cross each other and analysis domain has to be covered by the local meshes completely. If this condition is not satisfied, the satellite elements are referred to as inconsistent. After local mesh generation, the components of the global coefficient matrix associated with the P_i are calculated by integrating the entire satellite element around P_i. This process is repeated for all nodes. Finally, a global system of equation is obtained after all nodes have been integrated.

2.2 System Construction Considering Extensibility to Large DOF Analysis

In the proposed FMM, both pre-processing and main-processing can be parallelized in terms of nodes, where the pre-processing involves local mesh generation and the main-processing involves the construction and solution of system equations. Since the FMM follows the node-by-node procedure, the global matrix is constructed in a row-by-row manner and non-zero components of the global matrix in the row of a node are correspondent to the components derived from the satellite nodes. Thereby, the final system equations obtained by the node-by-node procedure are equivalent to that obtained by an element-by-element procedure mounted in conventional FEM.

On the other hand, some differences are arisen between the above two procedures when considering the further extensibility to large degree of freedom (DOF) analysis under the parallel computing environment. Fig. 3(a) shows schematics of the element-based domain decomposition during the parallel computing, where the global matrix is not constructed explicitly in most case whilst the parallel computing is performed on an element-by-element basis. Therefore, the node-based domain decomposition is employed in the proposed method like Fig. 3(b). As illustrated in the figure, nodes within the analysis domain are classified into two categories such as communication-independent nodes and communication-dependent nodes. The communication-independent nodes are defined as nodes that do not require communication between processors when the parallel computing is performed. Against to the communication-independent ones, the communication-dependent nodes are defined as nodes

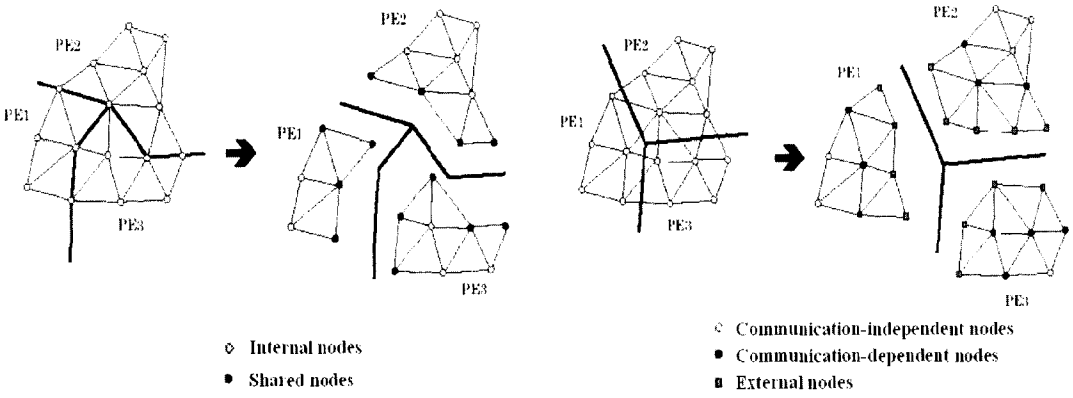

(a) Element-based partition (b) Node-based partition

Fig. 3 Domain decomposition for parallel computing

that require communication between processors. Generally, a parallel efficiency can be improved by dividing the nodes into these two categories. Since the efficiency of communication between processors depends on the numbering of nodal identifiers, in order to minimize the amount of communication, a parallel graph-partitioning library ParMETIS (http://www-users.cs.umn.edu/~karypis/metis, 2003) can be used for renumbering of the nodal identification numbers.

The node-by-node procedure described previously can be summarized as following seven steps:

(1) Read input data such as surface patches, coordinates of nodes and boundary conditions.

(2) Pick up a single node among all nodes and is designated as a central node.

(3) Generate local mesh around the central node.

(4) Calculate the components of the local coefficient matrix corresponding to the central node.

(5) Assemble the obtained components into the row of the global coefficient matrix corresponding to the central node.

(6) Obtain the complete components of the global coefficient matrix corresponding to the central node.

(7) Determine the complete global coefficient matrix.

In the above procedure, the step 2 is repeated for each node within the analysis domain and the step 4 is repeated for each satellite element associated with the central node.

3. Virtual Crack Closure Technique

3.1 Technical background of VCCT

For calculation of the energy release rate (G) and stress intensity factor (SIF, K), in general, fine FE meshes including crack-tip singular elements are required to get sufficiently accurate results. As an alternative to avoid the fine mesh, the use of small rosette around the crack-tip was proposed during original meshing and re-meshing when performing crack propagation analysis (Xie et al., 1995; Bocca et al., 1991; Wawrzynek and Ingraffea, 1989). This may lead to improved symmetry condition with respect to the crack and significant improvement of accuracy for coarse meshes. In the associated numerical studies, however, it was shown that the improvement was significantly dependent on the size of the rosette. Hence it is very difficult to determine which rosette size gives more accurate results in practice and, thereby, it severely constrains the applicability of this method.

The VCCT is one of attractive methods to overcome the limitations of cumbersome crack modeling through adopting non-singular crack-tip elements and to generate the FE meshes au-

tomatically. The three-dimensional VCCT is an extension of Rybicki-Kanninen method for two-dimensional crack configurations (Rybicki and Kanninen, 1977). It uses the fundamental assumption that any continuous function can be reasonably approximated by a finite number of straight line segments. By several researchers, the VCCT has been used for computing the energy release rates based on two- and/or three-dimensional FE analysis results under mixed-mode fracture condition (Rybicki and Kanninen, 1977; Raju, 1987).

Also, even though the original publication on VCCT dates back a quarter century, the VCCT has not yet been mounted into any of the generalized commercial FE codes such as MSC NASTRAN, ABAQUS and ANSYS etc. Instead of them, just FRANC2D developed by Cornell University and FAST developed by Tokyo Science University as non-commercial FE codes are publicly available ones adopting the VCCT (Ingraffea and Wawrzynek, 1995; Singh et al., 1998). That is, the VCCT has been used mainly by scientists in universities, research institutions and government laboratories and is usually implemented in their own specialized codes or post-processing routines in conjunction with commercial FE codes. However, recently, the interests on VCCT have been increased again in applied mechanics field to settle the mixed-mode fracture mechanics problems and damage tolerance assessment of composite structures etc.

3.2 Basic concept of VCCT (Krueger, 2002)

In a FE model consisted of eight-noded three-dimensional solid elements as shown in Fig. 4, the crack of length a is represented as a discontinuity by two surfaces. The additional dimension allows calculation for the distribution of the energy release rates along the crack front and makes it possible to obtain G_{III}, which is identical to zero for two-dimensional models. The nodes at top surface and bottom surface have identical coordinates and are not connected with each other as explained in the previous section. The crack front is represented by either a row of single nodes or two rows of nodes with

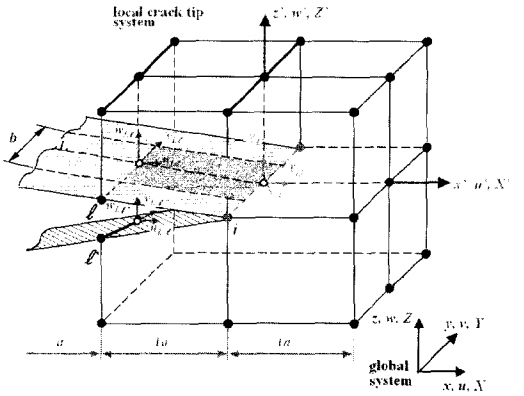

Fig. 4 Cracked model with bilinear three-dimensional solid elements

identical coordinates, coupled through multi-point constraints. The undamaged section, where the crack is closed and the structure is intact, is modeled using single nodes or two nodes with identical coordinates coupled through multi-point constraints if a crack propagation analysis is desired. The Model-I, Mode-II and Mode-III components of the energy release rates, G_I, G_{II} and G_{III} can be calculated by following equation.

$$G_I=\frac{1}{2\Delta A}\cdot Z_{Li}\cdot(w_{Ll}-w_{Ll}^*)$$
$$G_{II}=\frac{1}{2\Delta A}\cdot X_{Li}\cdot(u_{Ll}-u_{Ll}^*) \quad (1)$$
$$G_{III}=\frac{1}{2\Delta A}\cdot Y_{Li}\cdot(v_{Ll}-v_{Ll}^*)$$

where, $\Delta A=\Delta a\cdot b$ represents the area virtually closed (Δa is the length of the elements at the crack front and b is the width of the elements). X_{Li}, Y_{Li} and Z_{Li} denote the forces at the crack front in column L, row i. The corresponding displacements behind the crack at the top face node row l are denoted u_{kl}, v_{kl} and w_{kl}, and at the lower face node row l^* are denoted u_{kl}^*, v_{kl}^* and w_{kl}^*. All forces and displacements are obtained from the FE analysis with respect to the global system.

3.3 Application of VCCT

Fig. 5 illustrates the schematics of idealized

three-dimensional crack front to explain the determination of energy release rates. The accuracy of calculated values is primarily controlled by how well the crack front is segmented (Yagawa et al., 2003; Maiti, 1992). The energy release rates were determined after simplifying Equation (1) and by averaging the values at the selected nodes. The following equations were derived from the extension of two-dimensional equations and the calculated energy release rates are translated into a general form of SIFs.

$$G_i=\frac{1}{2S_i}\sum_{j=1}^{5} f_j^i \cdot u_j^i \quad (i: \text{Mode I, II, III}) \tag{2}$$

$$\begin{aligned} K_I &= \sqrt{E' G_I} \\ K_{II} &= \sqrt{E' G_{II}} \\ K_{III} &= \sqrt{2\mu G_{III}} \end{aligned} \tag{3}$$

where, i is fracture modes, j designates node number, f is a nodal force, a is a length of crack front element, S is a crack plane area, μ is a shear modulus, $E'=E/(1-\nu^2)$ for plane strain condition and $E'=E$ for plane stress condition.

On the other hand, in usual, relatively accurate conventional 2nd-order rectangular elements and hexahedral elements have been used for integrity evaluation of major components and structures as shown in Fig. 6(a). However, the generation of these types of elements requires a lot of times when comparing to that of triangular and tetrahedral elements. Also, it is very difficult and complex to generate both original and adaptive meshes automatically if users adopt additional nodes on element edges or inside elements whilst it may derive more exact results. Therefore, in this research, 1st-order triangular and tetrahedral elements are adopted and the applicability of them has been examined. Fig. 6 depicts the concept for application of three-dimensional VCCT using 1st-order tetrahedral elements. In order to calculate the energy release rate, 1st-order tetrahedral element group equivalent to the 2nd-order hexahedral elements was selected and substituted into Equation (2). For example, total forty eight times 1st-order tetrahedral elements (eight-folded in longitudinal direction and six-folded in thickness direction) were used instead of the equivalent 2nd-order hexahedral elements as shown in the figure.

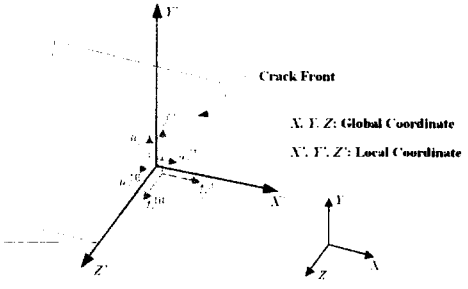

Fig. 5 Idealized crack front in VCCT

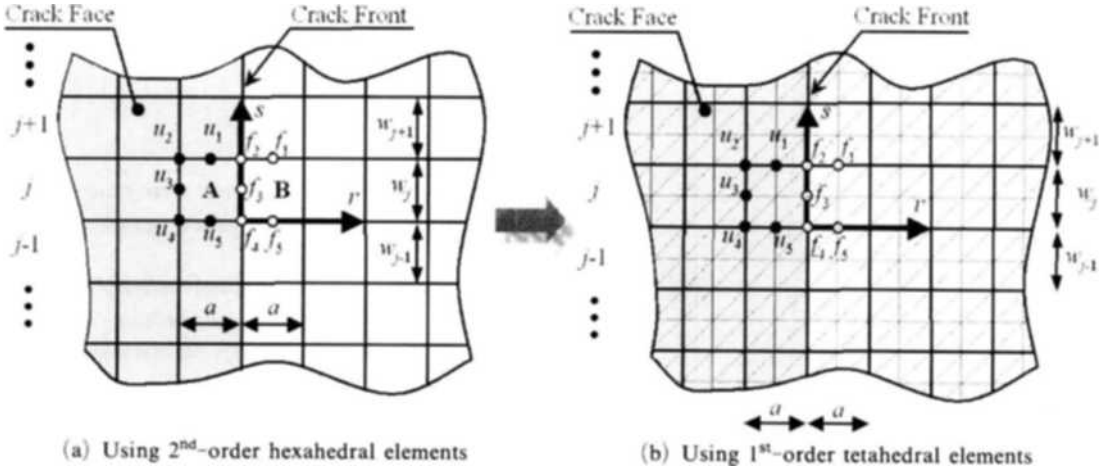

(a) Using 2nd-order hexahedral elements (b) Using 1st-order tetahedral elements

Fig. 6 Application of three-dimensional VCCT (Plane view)

4. Fracture Mechanics Analysis

4.1 Two-dimensional crack propagation analysis

To check the applicability of VCCT, two-dimensional quasi-static LEFM analyses using own FMM code developed by the authors were performed. The local FE mesh incorporating the triangular elements was robustly generated without any special treatment for crack-tips. As shown in Fig. 7, the surface patch data were firstly given to determine the boundaries of the object and then internal nodes were distributed across the domain. The nodes in the neighbourhood of the crack-tip were arranged using the special nodal pattern, which was moved as the crack propagation. The satellite elements associated with each node can be determined in a local manner using the coordinates of the neighbouring nodes and surface patch. The process of local mesh generation was repeated in accordance with the crack propagation.

Several crack propagation analyses have been carried out using the local finite element models for different geometries and loading conditions. The energy release rate (G) and SIF (K) that are known as representative fracture mechanics parameters were calculated. The values of G were obtained through the VCCT and translated to K according to following simplified two-dimensional equations (Shivakumar et al., 1988).

$$G_i=\frac{1}{2a\Delta t} f_i \cdot u_i \qquad (i: \text{Mode I, II}) \qquad (4)$$

$$K_i=\sqrt{G_i E'} \qquad (5)$$

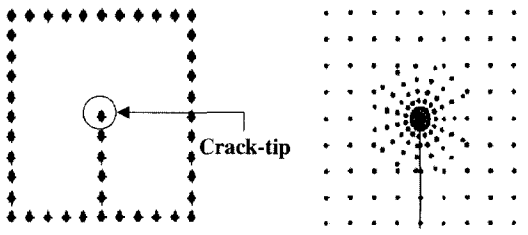

(a) Boundary nodes (b) Nodes around crack-tip

Fig. 7 Typical nodes for two-dimensional crack propagation analysis by FMM

where, i means fracture modes, f is a nodal force, a is a length of crack front element and E' represents a Young's modulus as shown in Fig. 8.

We can consider two typical crack propagation analysis models, i.e., Model A and Model B as depicted in Fig. 9. For the latter case, positions of new crack front nodes should be determined by propagation criterion. It includes the determination of the amount of crack extension and a kink angle (θ) as depicted in Fig. 10. Even

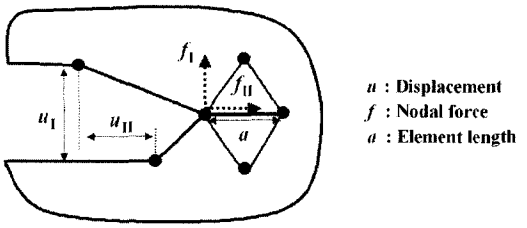

Fig. 8 Idealized finite element in VCCT

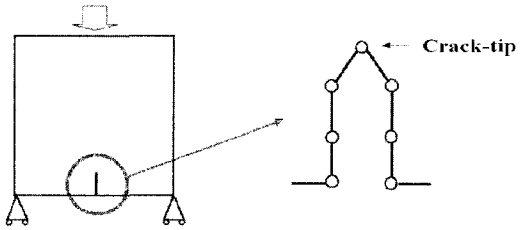

(a) Model A : Straight crack propagation

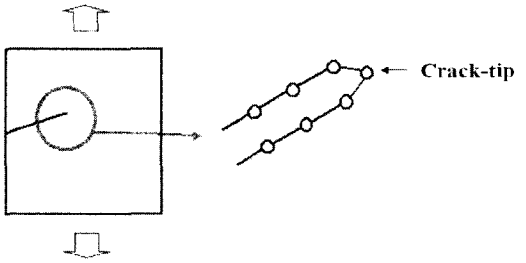

(b) Model B : Slant crack propagation

Fig. 9 Typical crack propagation analysis models

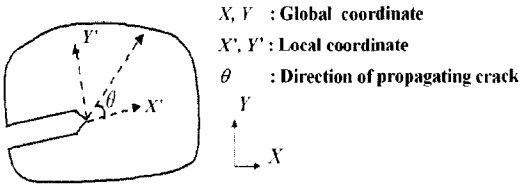

Fig. 10 Direction of crack propagation

though the modeling of crack propagation is one of interesting topics in fracture mechanics, it turns out to be difficult because of the re-meshing stage, which implies modifications of the mesh topology. In this section, the crack kink angle was determined by Equation (6) that was chosen among several crack propagation criteria such as the maximum tangential stress criterion, maximum energy release rate criterion and $K_{II}=0$ criterion etc (Khraisheh and Khan, 2000; Margevicius et al., 1999; Khan and Khraisheh, 2000; Rahman and Rao, 2002; Duarte et al., 2001; ABAQUS 2001).

$$\cos\frac{\theta}{2}[(K_I\sin\theta+K_{II}(3\cos\theta-1)]=0 \quad (6)$$

Figure 11 shows the schematics of crack-tip re-meshing for simulation of propagation in which two new nodes are generated at every analysis steps. Therefore, the crack propagations analyses can be available based on the fracture mechanics parameters obtained from Equations (4)~(6) and correspondent re-meshing process. Figs. 12 and 13 show the numerical examples of crack propagation analyses for edge cracked specimen with a crack and four point bend specimen with two cracks respectively. In these simulations, the local meshes were generated only where the connectivity between central nodes and associated satellite nodes were needed to be renewed. So, e.g., the local meshes were generated across the domain as shown in Fig. 13(a) and renewed only around the crack-tips like Fig. 13(b)~(d). In Fig. 13, the re-meshing parts were depicted as

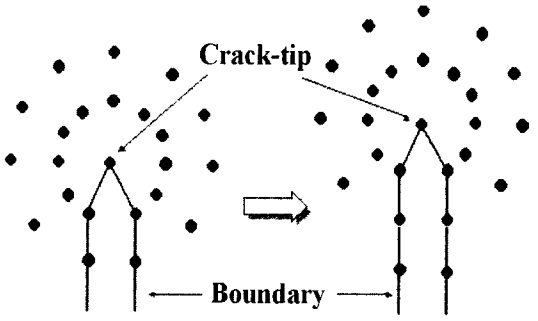

Fig. 11 Crack-tip re-meshing in two-dimensional crack propagation analysis

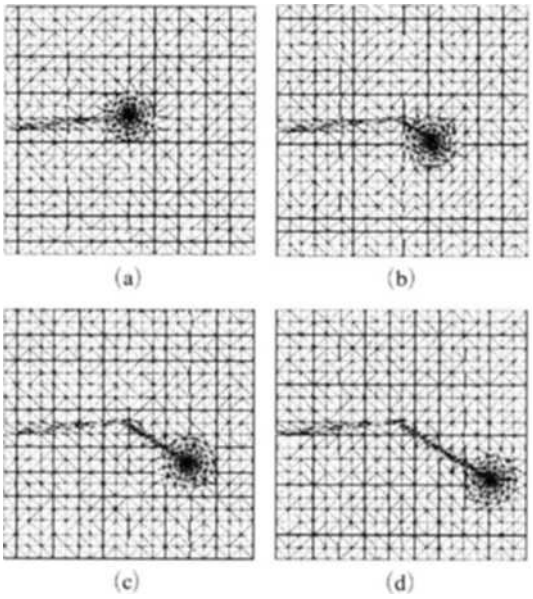

Fig. 12 Crack propagation analysis for edge cracked specimen

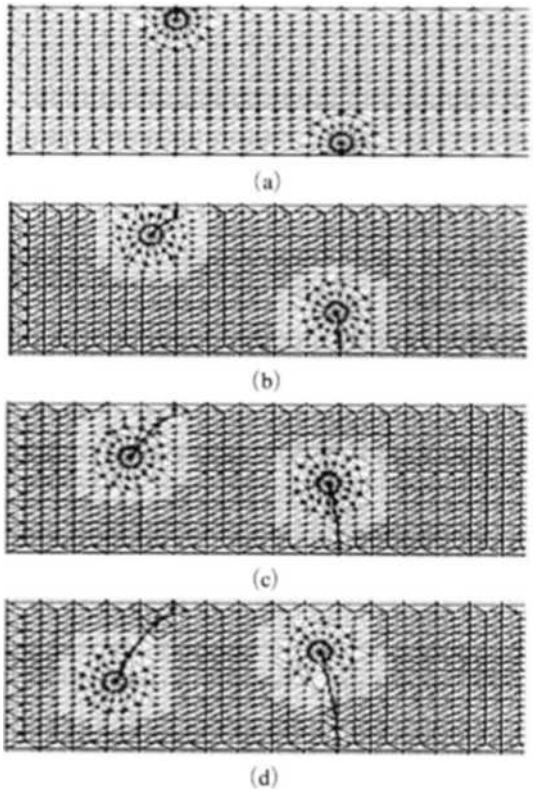

Fig. 13 Crack propagation analysis for four point bend specimen with two cracks

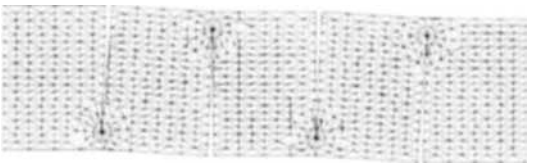

Fig. 14 Crack propagation analysis for multi-cracked TPB specimen

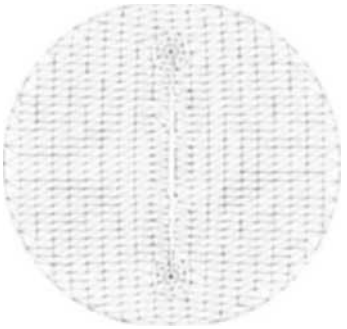

Fig. 15 Crack propagation analysis for Brazillian specimen

red lines. Figs. 14 and 15 show specimen models and crack propagation paths after the analyses for multi-cracked three point bend (TPB) and Brazillian specimens as the additional representative samples. The corresponding analyses results showed good applicability also.

4.2 Three-dimensional stable crack analysis

In order to check the additional validity of VCCT, a series of three-dimensional quasi-static LEFM analyses using own FEM code were carried out incorporating the 1st-order tetrahedral elements. In these analyses, the robust FE meshes were also generated without any special treatment for crack-tips. However, on the contrary to the two-dimensional analysis by FMM, the re-meshing was disregarded in this section since only stable crack evaluation for given cracks was considered. Fig. 16 shows the representative FE model for standard compact tension (1T-CT) specimen in which, the original crack lengths were changed sustaining the same shape of crack-tip region.

The calculated SIFs for full-model as well as half-model reflecting symmetric condition were

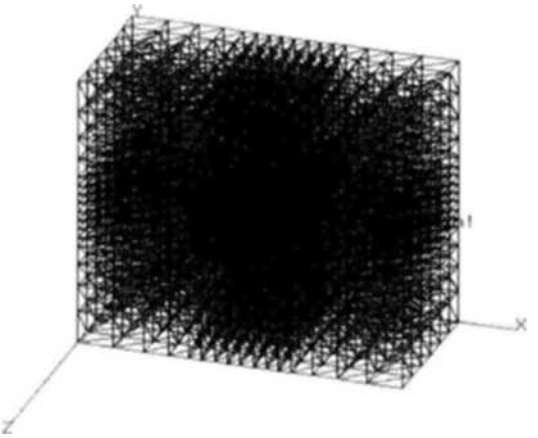

Fig. 16 Representative FE model for 1T-CT specimen

compared to the reference handbook solutions represented as Equation (7) (Murakami et al., 1987). In the analyses, 206 GPa of Young's modulus and 0.3 of Poisson's ratio that are typical nuclear piping material properties were used, and 3 kN of distributed loads were used as loading condition.

$$K_I = \frac{P}{tW^{1/2}} \cdot f_I(\alpha) \tag{7}$$

where,

$$f_I(\alpha) = \frac{(2+\alpha)(0.886+4.64\alpha-13.32\alpha^2+14.72\alpha^3-5.6\alpha^4)}{(1-\alpha)^{3/2}}$$

$$\alpha = \frac{a}{W}$$

Fig. 17 shows the SIF comparison results for varying crack length to specimen width ratios (a/W) under Mode-I condition in which the values of SIF were converted from the energy release rate data using Equation (2). As shown in the figure, it seems promising to use of the VCCT incorporating 1st-order tetrahedral elements for shallow- and standard- cracked geometries ($a/W=0.2\sim0.6$). However, for long-cracked geometries ($a/W=0.7\sim0.8$), differences between the calculated values and the reference solutions were increased and the reasons are being checked. Also, Fig. 18 shows representative numerical examples depicting von-Mises stress

distributions for $a/W=0.5$ under Mode-II and Mode-III conditions. A qualitative point of view, the stress distributions seems reasonable whilst those were not compared quantitatively since there were no corresponding reference solutions.

4.3 Discussion

In this research, the applicability of VCCT combined with FMM and FEM was examined incorporating the triangular elements for two-dimensional crack propagation analyses and the tetrahedral elements for three-dimensional stable crack evaluation. A series of prototypal analyses showed promising results, however, some incomplete portions were also derived that may act as obstacles for application of the current programs to industrial fields directly; fully random mesh generation near the crack-tip and treatment of large DOF stress analysis data in three-dimensional stable crack analysis etc.

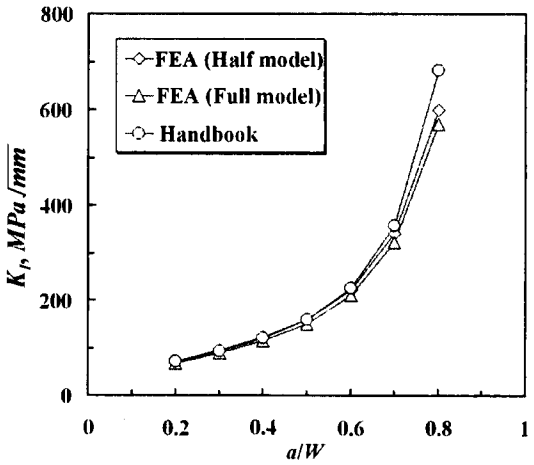

Fig. 17 SIF comparison results for 1T-CT specimens

In order to resolve the limitations, further researches are being considered. The representative one is a series of large DOF analyses for cylinder with four through-wall cracks that are inclined 45° against axes. Fig. 19 shows typical analysis model that consist of about 10^4 surface patches. During the analyses, crack lengths will be varied to find any effects between short crack and long crack. The loading condition will be decomposed into two loading types such as a torsional load (T) and tensile load (P). The validities of analyses results may demonstrated through comparisons to corresponding test results examined by other researchers (Yagawa et al., 2003). If the further researches were accomplished successfully, the VCCT can be applicable to industrial fields after finalization of interface part for user convenience.

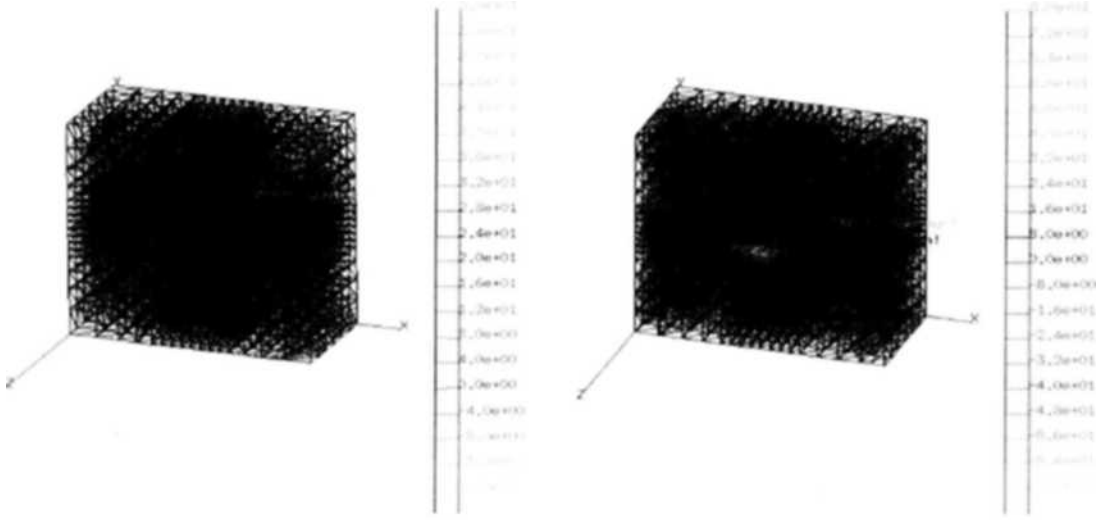

(a) Mode-II condition (b) Mode-III condition

Fig. 18 Representative von-Mises stress distributions for 1T-CT specimens

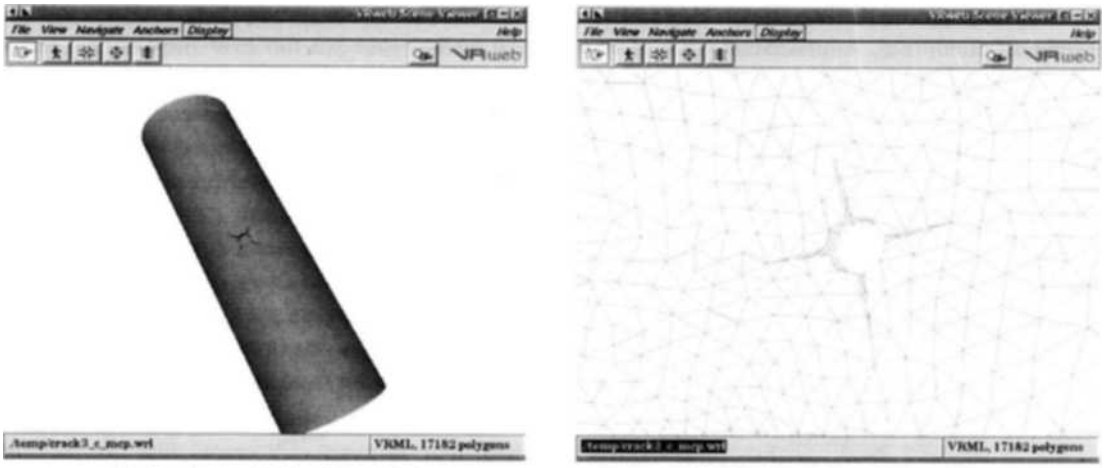

(a) Typical cylinder FE model (b) Enlarged cracked region

Fig. 19 Large DOF model considered in future research

5. Conclusion

A seamless analysis of material behaviour incorporating complex geometry and crack-tip modelling is one of interesting topic in engineering and computational fracture mechanics fields. In order to settle this issue, a numerical method to calculate an energy release rate by VCCT was proposed in this paper and following conclusions have been derived.

(1) An own code adopting VCCT combined with FMM was developed incorporating the triangular elements for two-dimensional crack propagation analyses. The applicability of VCCT has been examined via edge cracked specimen, four point bend specimen with two cracks, multi-cracked TPB specimen and Brazillian specimen etc. The crack propagation analyses results showed promising applicability.

(2) An own code adopting VCCT combined with FEM was examined incorporating the tetrahedral elements for a series of prototypal three-dimensional stable crack analyses. The applicability of VCCT has been examined via 1T-CT specimens with various a/W. The stable crack analyses results under Mode-I condition showed good applicability except for long-cracked geometries ($a/W=0.7\sim0.8$).

(3) The applicability of VCCT supported by the above promising results will be augmented through several ongoing researches such as fully random mesh generation near the crack-tip and treatment of large DOF stress analysis data etc.

Acknowledgment

The authors are grateful for the support provided by a grant from IML at the Tokyo University and Safety and Structural Integrity Research Centre at the Sungkyunkwan University.

References

ABAQUS Ver. 6.2, 2001, "User's Manual," Hibbitt, Karlsson & Sorensen Inc..

Belytschko, T. and Black, T., 1999, "Elastic Crack Growth in Finite Elements with Minimal Remeshing," *International Journal for Numerical Methods in Engineering*, Vol. 45, pp. 601~620.

Belytschko, T., Moes, N., Usui, S. and Parimi, C., 1999, "Arbitrary Discontinuity in Finite Elements," *International Journal for Numerical Methods in Engineering*, Vol. 50, pp. 993~1013.

Bocca, P., Carpinteri, A. and Valente, S., 1991, "Mixed-mode Fracture of Concrete," *International Journal of Solid Structure*, Vol. 27, No. 9, pp. 1139~1153.

Cho, J. Y. and Jee, Y. B., 2003, "An Adaptive Mesh-Independent Numerical Integration

for Meshless Local Petrov-Galerkin Method," *KSME International Journal*, Vol. 17, No. 7, pp. 986~998.

Choi, Y. J. and Kim, S. J., 2003, "Bending Analysis of Mindlin-Reissner Plates by the Element Free Galerkin Method with Penalty Technique," *KSME International Journal*, Vol. 17, No. 1, pp. 64~76.

Duarte, C. A. et al., 2001, "A Generalized Finite Element Method for the Simulation of Three-Dimensional Dynamic Crack Propagation," *Computer Methods in Applied Mechanics and Engineering*, Vol. 190, Nos. 15-17, pp. 2227~2262.

Inaba, M., Fujisawa, T. and Yagawa, G., 2002, "A New Algorithm of Local Mesh Generation for the Free Mesh Method," *Proceedings of JSME Dynamics and Design Conference*, p. 338.

Ingraffea, A. and Wawrzynek, P., 1995, "FRANC2D : A Case Study in Transfer of Software Technology, in Research Transformed into Practice," *ASCE Press*.

Jin, C. and Suzuki, K., 2000, "Methodology and Property of Cover Least Square Approximation," *Transactions of the Japan Society for Computational Engineering and Science*, Vol. 2, pp. 213~218.

Khan, S. M. A. and Khraisheh, M. K., 2000, "Analysis of Mixed Mode Crack Initiation Angles under Various Loading Conditions," *Engineering Fracture Mechanics*, Vol. 67, No. 5, pp. 397~419.

Khraisheh, M. K. and Khan, S. M. A., 2000, "Maximum Stress Triaxiality Ratio Criterion for Mixed Mode Crack Initiation in Anisotropic Materials," *International Journal of Fracture*, Vol. 104, No. 3, pp. 11~16.

Krueger, R., 2002, "The Virtual Crack Closure Technique : History, Approach and Application," NASA/CR-2002-211628.

Maiti, S. K., 1992, "Finite Element Computation of Crack Closure Integrals and Stress Intensity Factors," *Engineering Fracture Mechanics*, Vol. 41, No. 3, pp. 339~348.

Margevicius, R. W., Riedle, J. and Gumbsch, P., 1999, "Fracture Toughness of Polycrystalline Tungsten under Mode I and Mixed Mode I/II Loading," *Materials Science and Engineering*, Vol. A270, pp. 197~209.

Melenk, J. M. and Babuska, I., 1996, "The Partition of Unity Finite Element Method : Basic Theory and Applications," *Computer Methods in Applied Mechanics and Engineering*, Vol. 139, pp. 289~314.

Murakami, Y. et al., 1987, "Stress-Intensity Factors Handbook," Vol. 1, Pergammon Press, Tokyo.

Rahman, S. and Rao, B. N., 2002, "Probabilistic Fracture Mechanics by Galerkin Meshless Methods — Part II : Reliability Analysis," *Computational Mechanics*, Vol. 28, No. 5, pp. 365~374.

Raju, I. S., 1987, "Calculation of Strain Energy Release Rates with Higher Order and Singular Finite Elements," Engineering Fracture Mechanics, Vol. 28, No. 3, pp. 251~274.

Rybicki, E. F. and Kanninen, M. F., 1977, "A Finite Element Calculation of Stress Intensity Factors by a Modified Crack Closure Integral," *Engineering Fracture Mechanics*, Vol. 9, No. 8, pp. 931~938.

Shivakumar, A. K., Tan, P. W. and Newman, J. C. Jr., 1988, "A Virtual Crack-closure Technique for Calculating Stress Intensity Factors for Cracked 3-dimensional Bodies," *International Journal of Fracture*, Vol. 36, R43-R50.

Singh, R. et al., 1998, "Universal Crack Closure Integral for SIF Estimation," *Engineering Fracture Mechanics*, Vol. 60, No. 2, pp. 133~146.

Wawrzynek, P. A. and Ingraffea, A. R., 1989, "An Interactive Approach to Local Remeshing Around a Propagation Crack," *Finite Element Analysis Design*, Vol. 5, pp. 87~96.

Xie, M., Gerstle, W. H. and Rahulkumar, P., 1995, "Energy-based Automatic Mixed-mode Crack Propagation Modeling," *Journal of Engineering Mechanics ASCE*, Vol. 121, No. 8, pp. 914~923.

Yagawa, G. and Yamada, T., 1996, "Free Mesh Method : A New Meshless Finite Element Method," *Computational Mechanics*, Vol. 18, No. 5, pp. 383~386.

Yagawa, G. and Furukawa, T., 2000, "Recent

Development of Free Mesh Method," *International Journal for Numerical Methods in Engineering*, Vol. 17, pp. 1419~1443.

Yagawa, G. et al., 2003, "Research on Fatigue Properties under Multi-axial State of Stress," Japan Welding Engineering Society.

http://www-users.cs.umn.edu/~karypis/metis, "Family of Multilevel Partitioning Algorithms," 2003.